J Wood Sci (2007) 53:168–174
DOI 10.1007/s10086-006-0834-z

NOTE

Haruo Kawamoto · Sunao Horigoshi · Shiro Saka

Pyrolysis reactions of various lignin model dimers

Received: March 20, 2006 / Accepted: July 26, 2006 / Published online: Decebmer 2, 2006

Abstract Primary pyrolysis reactions and relative reactivities for depolymerization and condensation/carbonization were evaluated for various lignin model dimers with *α-O*-4, *β-O*-4, *β*-1, and biphenyl substructures by characterizing the tetrahydrofuran (THF)-soluble and THF-insoluble fractions obtained after pyrolysis at 400°C. Reactivity was quite different depending on the model structure: depolymerization: *α-O*-4 [phenolic (ph), nonphenolic (nonph)], *β-O*-4 (ph) > *β-O*-4 (nonph), *β*-1 (ph, nonph) > biphenyl (ph, nonph); condensation/carbonization: *β*-1 (ph) > *β-O*-4 (ph) > *α-O*-4 (ph) > *β-O*-4 (nonph), biphenyl (ph, nonph), *α-O*-4 (nonph), *β*-1 (nonph). Major degradation pathways were also identified for *β-O*-4 and *β*-1 model dimers: *β-O*-4 types: C_β-O cleavage to form cinnamyl alcohols and phenols and C_γ-elimination yielding vinyl ethers; *β*-1 types: C_α-C_β cleavage yielding benzaldehydes and styrenes and C_γ-elimination yielding stilbenes. Relative reactivities of these pathways were also quite different between phenolic and nonphenolic forms even in the same types; C_β-O cleavage (*β-O*-4) and C_γ-elimination (*β*-1) were substantially enhanced in phenolic forms.

Key words Pyrolysis · Pyrolysis behavior · Lignin · Model compound · Degradation pathway

Introduction

Pyrolysis is the underlying principle of various thermochemical conversion processes including fast pyrolysis for bio-oil production, gasification, and carbonization. However, product selectivity in wood pyrolysis is usually low and produces a complex mixture of gaseous, liquid, and solid carbonized products. Low product selectivity sometimes causes negative effects on the product utilization, for example, tar trouble in wood gasification, as well as lowering the conversion efficiency.

The molecular mechanism of wood pyrolysis very important in terms of understanding and improving the product selectivity. For cellulose, Kawamoto et al.[1–3] proposed that the ring-opening polymerization of levoglucosan, the major primary pyrolysis product, to be a key reaction that determines the product selectivity between low molecular weight (MW) products and solid carbonized products. Selective conversion of cellulose to low MW[2] and some useful chemicals[4] were also demonstrated by pyrolysis in sulfolane solvent.

However, knowledge of lignin pyrolysis is very limited except for the studies of the weight-loss behavior and characterization of the low MW products. Weight loss of lignin during heating in nitrogen has been reported with thermogravimetric analysis to occur gradually in a wide range of temperature between 200° and 500°C with a substantial amount of residue remaining compared with wood polysaccharides.[5] Evolution of some low MW products including simple phenols, formic acid, formaldehyde, methanol, carbon monoxide, and water have been reported with thermofractography,[6,7] Fourier transform infrared (FT-IR)-evolved gas analysis,[8] and thermogravimetry/mass spectrometry.[9,10] Pyrolysis residues from lignin were also characterized with spectroscopic techniques including IR and cross polarization/magic-angle spinning nuclear magnetic resonance (CP/MAS NMR) spectroscopy. Haw and Schultz[11] analyzed the pyrolyzed residues obtained from some isolated lignins with CP/MAS NMR spectroscopy and they reported that the *β-O*-4 structure starts to decompose at a temperature as low as 220°C. Although these studies give useful information about the weight-loss behavior and properties of volatiles and residues, there is little information about the chemical reactions involved in lignin pyrolysis.

Lignin is a heterogeneous polymer consisting of phenylpropane units linked through various ether and C-C linkages. Thus, understanding the pyrolysis reactions of

H. Kawamoto (✉) · S. Horigoshi · S. Saka
Department of Socio-Environmental Energy Science, Graduate School of Energy Science, Kyoto University, Yoshida Hon-machi, Sakyo-ku, Kyoto 606-8501, Japan
Tel. +81-75-753-4737; Fax +81-75-753-4737
e-mail: kawamoto@energy.kyoto-u.ac.jp

these substructures is quite important for understanding the overall lignin pyrolysis. As for pyrolysis behavior of the lignin substructure, thermogravimetric studies of various lignin model compounds were conducted by Domburg and his coworkers.[12–14] Several articles also reported the pyrolytic products from lignin model compounds. Klein and Virk[15] reported the formation of styrene and phenol from pyrolysis of phenethyl phenyl ether and proposed a retro-ene mechanism for the pyrolytic β-ether cleavage. Brežný et al.[16] reported the pyrolytic products from guaiacylglycerol β-guaiacyl ether and its derivatives and the formation of these products were explained with an oxirane mechanism. Thus, knowledge of the degradation pathway and reactivity of lignin substructure is very limited.

In this article, the primary pyrolysis reaction and relative reactivity for depolymerization and condensation/carbonization at 400°C studied with α-ether, β-ether, β-1, and biphenyl types of lignin model dimers are presented. The role of the substructure in overall lignin pyrolysis is also discussed with the present results.

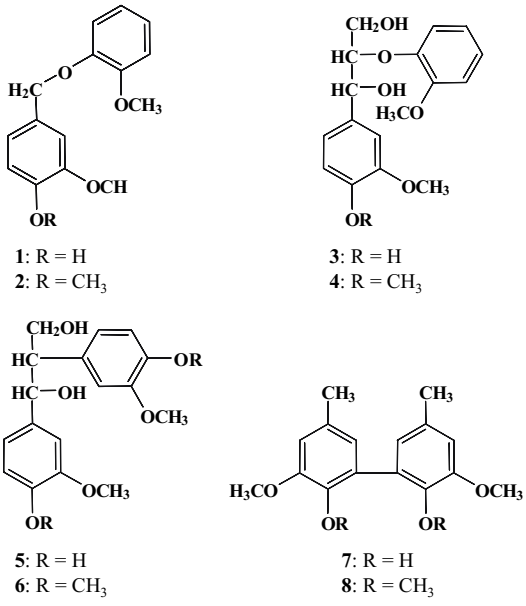

Fig. 1. Model dimers used in the experiments

Experimental

Pyrolysis products were separated by using preparative thin-layer chromatography (TLC) on silica gel plates (Kieselgel 60 F_{254}, Merck). Ultraviolet (UV) spectra were taken with a Shimadzu UV-2400 spectrometer. High performance liquid chromatography (HPLC) was conducted with a Shimadzu LC-10A under the following chromatographic conditions: column, STR ODS-II; flow rate, 0.7 ml/min; eluent, MeOH/H_2O = 30/70 → 100/0 (0 → 40 min), 100/0 (40 → 50 min); detection at 254 nm; 40°C. Gel permeation chromatography (GPC) was conducted with a Shimadzu LC-10A under the following chromatographic conditions: column, Shodex KF-801 (exclusion limit: MW 1500, polystyrene); flow rate, 1.0 ml/min; eluent, tetrahydrofuran (THF), detection at 254 nm; 40°C. ^{1}H-NMR spectra were recorded in $CDCl_3$ with a Varian AC-300 (300 MHz) spectrometer with tetramethylsilane (TMS) as an internal standard. Chemical shift (δ) and coupling constant (J) are given in ppm and Hz, respectively.

Model compounds

Lignin model dimers **1**–**8** were selected as model compounds for α-*O*-4, β-*O*-4, β-1, and biphenyl structures in lignin (Fig. 1). Lignin model dimers **1**–**8** represent a large part of the structure of softwood lignin; the contents of the substructures are reported for spruce milled wood lignin (MWL) as:[17] ether structure β-*O*-4 (48), noncyclic α-*O*-4 (6–8), 5-*O*-4 (3.5–4); condensed structure 5-5 (9.5–11), β-1 (7), condensed structures in 2- or 6-position (2.5–3), β-β (2); mixed structure phenylcoumaran (β-5, α-*O*-4) (9–12), where the numbers in parentheses indicate the number of the substructure in lignin consisting of 100 phenylpropane units. Dimers **5** and **6** (β-1 types) are considered to be useful for other C_β-C_{aryl} types of structures.

2-Methoxy-4-[(2-methoxyphenoxy)methyl]phenol (**1**), was prepared by condensation of 4-benzyloxy-3-methoxybenzyl bromide with excess guaiacol in the presence of potassium carbonate in DMF, followed by hydrogenation over 10% Pd-C in THF/$CHCl_3$. 1,2-Dimethoxy-4-[(2-methoxyphenoxy)methyl]benzene (**2**) was prepared by a similar condensation reaction of 3,4-dimethoxybenzyl bromide with excess guaiacol. 4-Benzyloxy-3-methoxybenzyl bromide and 3,4-dimethoxybenzyl bromide were prepared by bromination of the corresponding vanillyl alcohol derivatives with 47% HBr in $CHCl_3$. Compound **1**: ^{1}H-NMR ($CDCl_3$, 300 MHz) δ: 3.88 (3H, s, —OCH_3), 3.89 (3H, s, —OCH_3), 5.06 (2H, s, C_α-H), 6.9–7.0 (7H, m, aromatic H). Compound **2**: ^{1}H-NMR ($CDCl_3$, 300 MHz) δ: 3.85 (3H, s, —OCH_3), 3.86 (6H, s, —OCH_3), 5.07 (2H, s, C_α-H), 6.8–7.0 (7H, m, aromatic H).

1-(4-Hydroxy-3-methoxyphenyl)-2-(2-methoxyphenoxy)-1,3-propanediol (guaicylglycerol-β-guaicyl ether) (**3**) and 1-(3,4-dimethoxyphenyl)-2-(2-methoxyphenoxy)-1,3-propanediol (veratrylglycerol-β-guaiacyl ether) (**4**) were prepared according to the procedure described by Nakatsubo et al.[18] 1,2-Bis(4-hydroxy-3-methoxyphenyl) propane-1,3-diol (**5**)[19] and 1,2-bis(3,4-dimethoxyphenyl) propane-1,3-diol (**6**)[20] were prepared according to the procedures reported by Lundquist's group. 2,2′-Dihydroxy-3,3′-dimethoxy-5,5′-dimethyl biphenyl (**7**) and 2,2′,3,3′-tetramethoxy-5,5′-dimethyl biphenyl (**8**) were prepared according to the method described by Kratzl and Vierhapper.[21]

Pyrolysis and product characterization

Pyrolysis of each lignin model compound was conducted with an apparatus consisting of a round flask (volume 20 ml) with a glass tube (120 mm long and 14 mm in diameter) for trapping the volatile products with a nitrogen bag through a

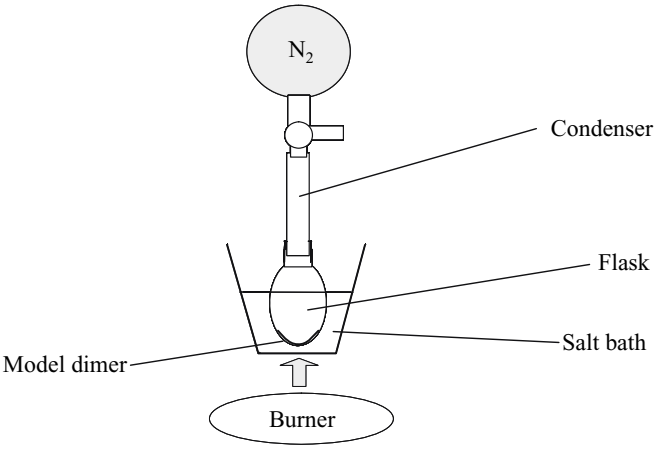

Fig. 2. Experimental setup used for pyrolysis of model dimers

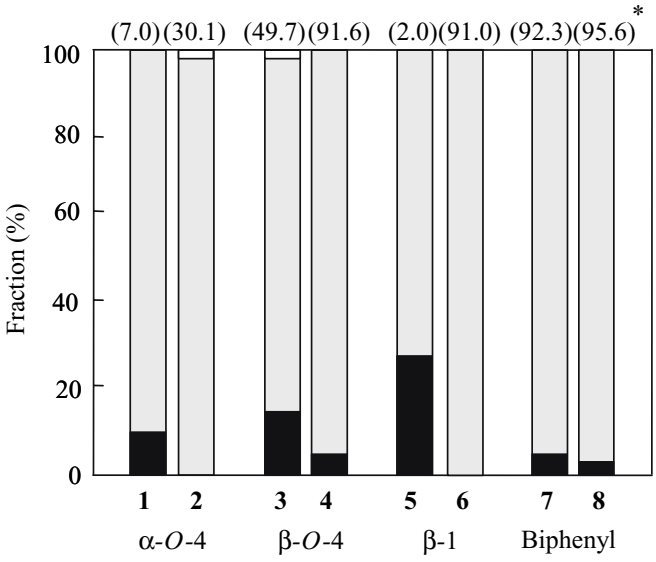

Fig. 3. Fractional composition of the pyrolysis mixture and recovered yield of model dimer under the pyrolysis conditions (N_2/400°C/1 min). *Open bars*, gaseous fraction; *shaded bars*, tetrahydrofuran (THF)-soluble fraction; *filled bars*, THF-insoluble fraction; *asterisk*, percent recovered yields of model dimer

three-way tap as shown in Fig. 2. Model compound (10 mg) was placed at the bottom of the flask as a thin film by evaporating the solution in MeOH (2.0 ml), and the flask attached with the other apparatus was heated for 1 min in a salt bath ($KNO_3/NaNO_3$ = 1/1, w/w) preheated at 400°C after replacing the air in the reaction system with nitrogen. Although heating rate was not evaluated, temperature of the flask was expected to be raised quickly in this experiment. Under these pyrolysis conditions, major pyrolysis reactions of model dimers were completed. After the pyrolysis, the flask was immediately cooled with air flow for 30 s and subsequently in cold water for 3 min. Then the reaction system was opened to release the gaseous products, and the flask and glass tube were extracted with THF (5.0 ml × 2) to give THF-soluble and THF-insoluble fractions. The amounts of gaseous, THF-soluble, and THF-insoluble fractions were determined with the weight difference of the glassware before and after opening or extraction. THF-soluble fractions were analyzed with GPC and HPLC. Products were identified by comparing the ^{1}H-NMR spectra of the isolated products with those of the authentic compounds and were quantified with HPLC.

Results and discussion

Fractional composition and relative reactivity

Figure 3 summarizes the fractional composition and recovered yields of the model dimers under the pyrolysis conditions (N_2/400°C/1 min). THF-insoluble fractions (0%–32% yields) with dark-brown to black appearance were obtained. THF-soluble fractions (72%–100%) that were colorless to light yellow in color included the unreacted model dimers. Evolution of the gaseous products was very limited under the conditions used. The THF-insoluble fractions were not soluble in common solvents such as methanol, ethanol, dioxane, DMF, or dimethyl sulfoxide (DMSO) and are defined in this article as carbonization products.

The recovered yield of model dimer was quite different depending on the structure. Reactivity indicated from the recovered yield was in the order of phenolic β-1 (**5**) (2.0) > phenolic α-*O*-4 (**1**) (7.0) > nonphenolic α-*O*-4 (**2**) (30.1) > phenolic β-*O*-4 (**3**) (49.7) > nonphenolic β-1 (**6**) (90.5), nonphenolic β-*O*-4 (**4**) (91.6), phenolic biphenyl (**7**) (92.3), and nonphenolic biphenyl (**8**) (95.6) (where the numbers in parentheses represent percent recovered yield). Generally, phenolic forms (**1**, **3**, **5**, and **7**) are more reactive than the corresponding nonphenolic forms (**2**, **4**, **6**, and **8**). Yields of the THF-insoluble fractions, which were also different between model dimers, were roughly related to the reactivity of model dimers.

Degradation pathway

Gel permeation chromatograms of the THF-soluble fractions are summarized in Fig. 4. Each asterisk in Fig. 4 indicates the retention time of the relevant model dimer. Except for the α-ether types, products with MW larger than the model dimers are scarcely observed in the chromatograms in spite of the formation of the THF-insoluble (carbonization) fractions. Because THF is considered to solubilize products with a wide range of MW, the THF-insoluble (carbonization) fraction is indicated to be formed via some very reactive intermediate without leaving the condensation products soluble in THF. The chromatograms in Fig. 4 also indicate that lower MW products are formed from the dimers other than biphenyl types **7** and **8**, which show only single peaks corresponding to the model dimers. Structures of the lower MW products were characterized by ^{1}H-NMR analysis of the isolated products.

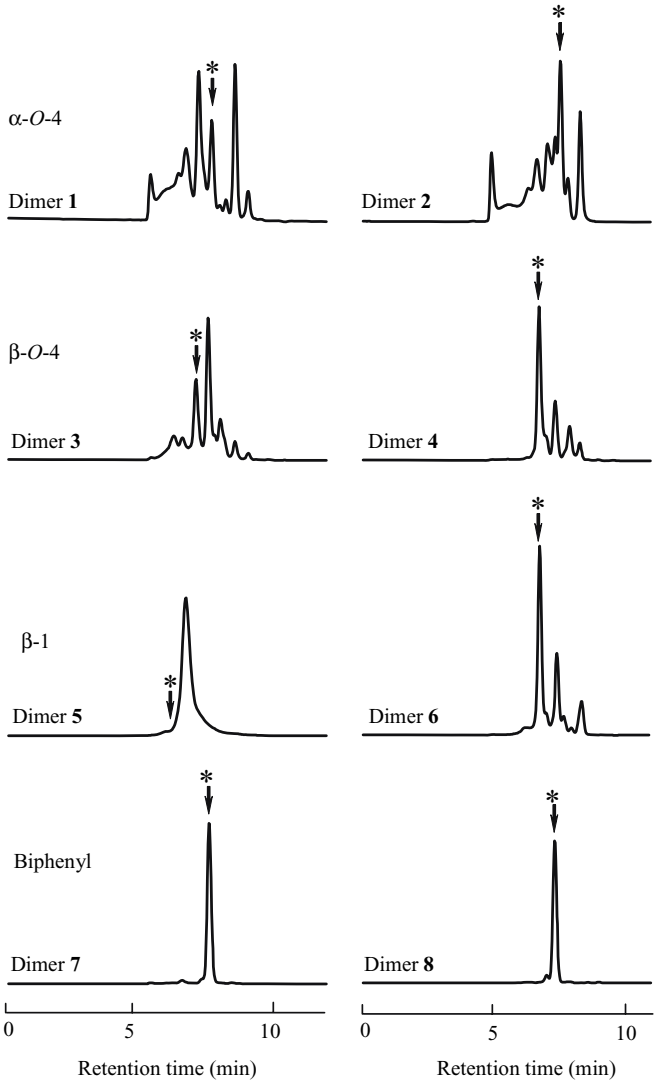

Fig. 4. Chromatograms from gel permeation chromatography of the THF-soluble fractions. *Asterisk* highlights the peak and retention time of each model dimer

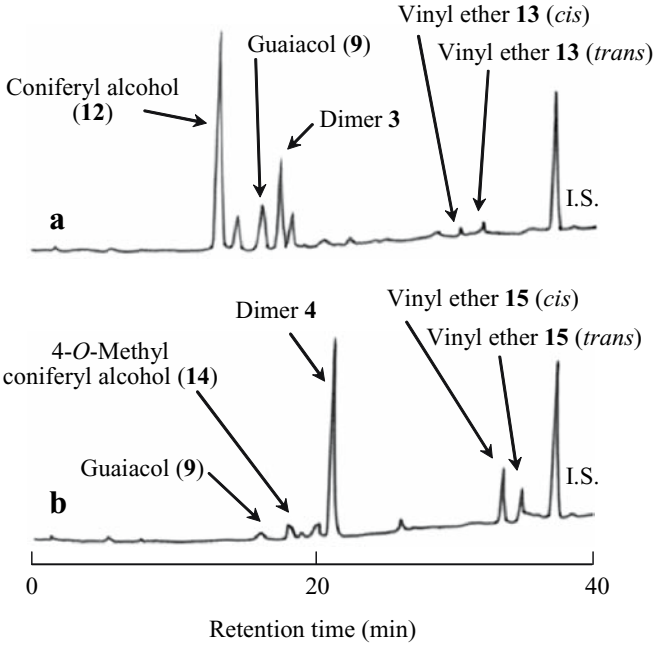

Fig. 5a, b. Chromatograms from high performance liquid chromatography (HPLC) of the THF-soluble fractions obtained from the *β-O*-4-type model dimers **3** and **4**. **a** Phenolic dimer **3**, **b** nonphenolic dimer **4**

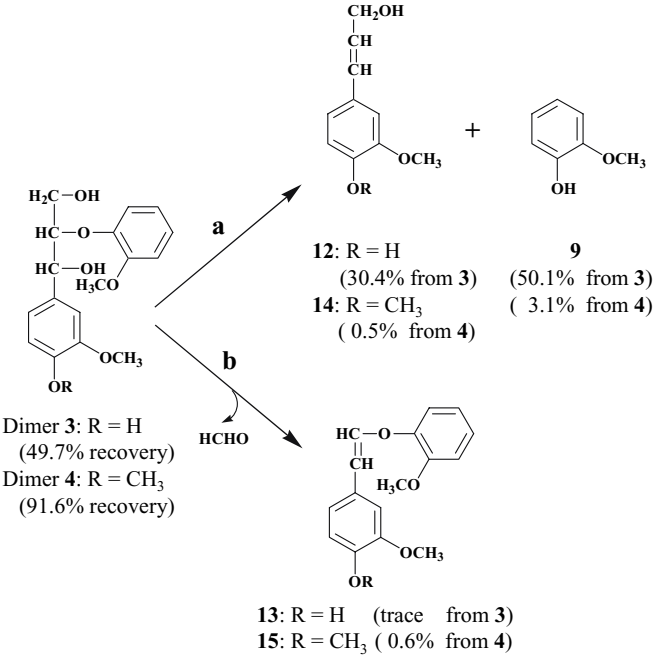

Fig. 6. Pyrolytic pathways **a** and **b** of the *β-O*-4-type model dimers **3** and **4**

α-O-4 Dimers

α-O-4-Type model dimers **1** and **2** gave 2-methoxyphenol (guaiacol) (**9**) in 68.1% and 43.6% yields, respectively, which is evidence of the *α*-ether cleavage, with a variety of other unidentified products. This indicates that *α*-ether linkages in both phenolic and nonphenolic forms are easily cleaved at 400°C. The cleavage mechanism is not clear at present, although an ionic mechanism via a quinone methide intermediate and radical mechanism can be considered.

β-O-4 Dimers

Cinnamyl alcohols, vinyl ethers, and guaiacol were identified as degradation products from the *β-O*-4-type model dimers **3** and **4** (Fig. 5). From phenolic dimer **3** (49.7% recovery), considerable amounts of 2-methoxy-4-[2-(2-methoxyphenoxy)ethenyl]phenol (coniferyl alcohol) (**12**) (30.4%) and guaiacol (**9**) (50.1%) were obtained with a trace amount of a vinyl ether, 1-(4-hydroxy-3-methoxyphenyl)-2-(2-methoxyphenoxy)ethene (**13**). On the other hand, much lower yields of 4-*O*-methylconiferyl alcohol (**14**) (0.5%) and guaiacol (**9**) (3.1%) were obtained from the nonphenolic dimer **4** (recovered yield: 91.6%)

with a vinyl ether, 1-(3,4-dimethoxyphenyl)-2-(2-methoxyphenoxy)ethene (**15**) (*cis*:*trans* = 2:1) (0.6%). All the products were identified by comparing the ^{1}H-NMR spectra of the isolated compounds with those of the authentic compounds as well as by comparison of the retention times in HPLC analysis.

Structures of the degradation products indicate two types of reactions: C_β-O cleavage yielding cinnamyl alcohols and guaiacol (pathway **a**) and C_γ-elimination forming vinyl ethers (pathway **b**) occurring in both phenolic and nonphenolic structures (Fig. 6). In pathway **b**, γ-carbon is considered to be eliminated as formaldehyde. Formaldehyde formation during lignin pyrolysis has been reported by many researchers.[8–10]

Comparison of the guaiacol yields (50.1% and 3.1% from compounds **3** and **4**, respectively) as evidence of the β-ether cleavage indicates that the phenolic structure is much more reactive for β-ether cleavage than the nonphenolic structure. These results are consistent with the results reported by Domberg et al.[13] and Brežný et al.[16] They reported that phenolic β-ether structure was cleaved at a much lower temperature than the nonphenolic structure. The much higher yield of coniferyl alcohol (**12**) (30.4%) from phenolic dimer **3** than that (0.5%) of 4-*O*-methyl coniferyl alcohol (**14**) from nonphenolic dimer **4** suggests that reactivity in pathway **a** is much higher in the phenolic form than the nonphenolic form.

In pyrolyzing vinyl ethers **13** (*cis*:*trans* = 1:1) and **15** (*cis*:*trans* = 1:1), which were prepared according to the procedure reported by Yaguchi et al.,[22] under the same pyrolysis conditions (N_2/400°C/1 min), compound **13** gave guaiacol (**9**) (29.7%) and THF-insoluble products (23.0%) with unreacted compound **13** (8.4%), while compound **15** gave only a trace amount of guaiacol (**9**). These results indicate that β-ether cleavage also proceeds from the phenolic vinyl ether intermediate **13**, although contribution of this pathway is not clear at the moment. Vanillin and veratraldehyde, which are considered to be formed through Cα-Cβ cleavage, were not detected from dimers **3** and **4**.

Brežný et al.[16] already reported the products obtained from model dimer **3** by heating to 275°C at a heating rate of 10°C/min, but their products were a complex mixture of guaiacol (6.4%), coniferyl alcohol (4.3%), coniferyl aldehyde (3.8%), guaiacyl vinyl ketone (3.8%), 1-(4-hydroxy-3-methoxyphenyl)-3-hydroxy-1-propanone (2.2%), and vanillin (0.5%) with much lower yields than in this study. These differences are considered to be derived from the experimental conditions used. Slow heating conditions in the sealed reactor used in the study of Brežný et al.[16] enhance the secondary reactions of the primary products. On the other hand, the experimental setup used in this study (Fig. 2) offers high heating rate conditions and effective removal of the low MW products from the heated zone, and these effectively suppress the secondary reactions.

Consequently, for the β-*O*-4 structure, two types of reactions, C_β-O cleavage and C_γ-elimination, were suggested as important pyrolytic reactions. Furthermore, the former reaction was found to be enhanced substantially in phenolic form.

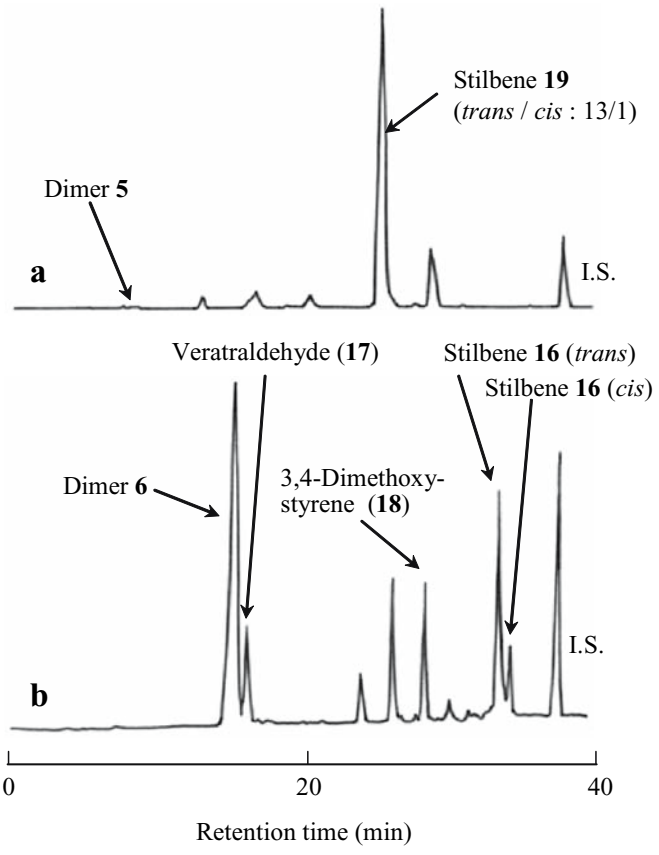

Fig. 7a, b. HPLC chromatograms of the THF-soluble fractions obtained from the β-1-type model dimers **5** and **6**. **a** Phenolic dimer **5**, **b** nonphenolic dimer **6**

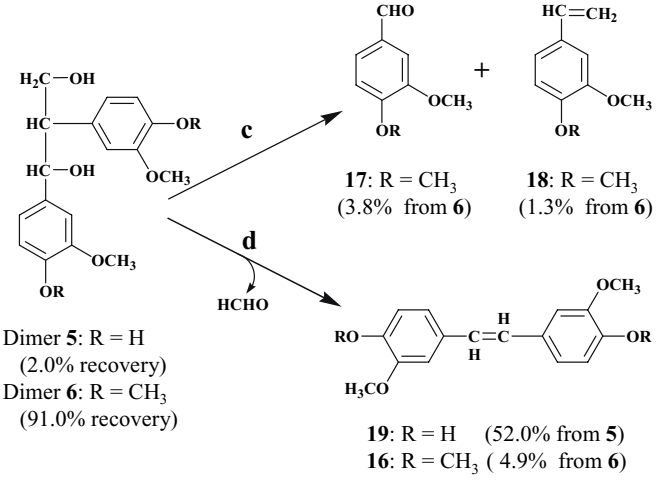

Fig. 8. Pyrolytic pathways **c** and **d** of the β-1-type model dimers **5** and **6**

C_β-C_{aryl} Dimers

Stilbene, benzaldehyde, and styrene were identified from the β-1-type model dimers **5** and **6** (Fig. 7). These products indicate two pyrolytic pathways in the pyrolysis of the β-1 types; one is the C_α-C_β cleavage to yield benzaldehyde and

styrene (pathway **c**), and the other is the C_γ-elimination to form stilbene (pathway **d**) (Fig. 8). Furthermore, yields of these products suggest that relative importance of these pathways is different between phenolic and nonphenolic forms.

Nonphenolic dimer **6** gave 3,3′,4,4′-tetramethoxystilbene (**16**) (*trans*:*cis* = 4:1), veratraldehyde (**17**), and 3,4-dimethoxystyrene (**18**) in 4.9%, 3.8% and 1.3% yields, respectively. On the other hand, phenolic dimer **5** predominantly gave 4,4′-dihydroxy-3,3′-dimethoxystilbene (**19**) (*trans*:*cis* = 13:1) (52.0%), and the corresponding benzaldehyde and styrene were not detected in the pyrolyzate. Products **17** and **18** were identified by comparison of their ^{1}H-NMR spectra with those of the authentic compounds. Stilbenes **16** and **19** were identified with their ^{1}H-NMR[23] and UV[24] spectra. These results indicate that the C_α-C_β cleavage and the C_γ-elimination proceed to a similar extent for nonphenolic dimer **6**, and that the C_γ-elimination predominantly occurs in the phenolic dimer **5**. These differences may be attributed to the quinone methide formation in the phenolic form, although further study is necessary to discuss the mechanism. In terms of depolymerization of lignin chain structure, nonphenolic C_β-C_{aryl} structure is rather effective through C_α-C_β cleavage (pathway **c**) compared with the phenolic structure. The phenolic structure is selectively converted to stilbene through C_γ-elimination (pathway **d**). These results are also supported by the GPC chromatograms in Fig. 4. Although only one peak corresponding to stilbene **19** is observed in the chromatogram of phenolic dimer **5**, two clear peaks of stilbene **16** and compounds **17** and **18** are observed in the chromatogram of nonphenolic dimer **6**.

Biphenyl dimers

Only unreacted biphenyl-type dimers **7** and **8** were observed in HPLC chromatograms. These results indicate that biphenyl structure such as 5–5 linkage is stable for depolymerization even at 400°C. However, THF-insoluble fractions were obtained in 4.0% and 2.0% yields, respectively (Fig. 3). This indicates that carbonization also occurs in these dimers.

Role of substructure on lignin pyrolysis at 400°C

Figure 9 summarizes the relative reactivity of the model dimers for depolymerization and condensation/carbonization. Reactivity for depolymerization is shown as the yield of the depolymerized products. The depolymerized product is defined here as a product obtained from breaking of the linkage between two aromatic rings, and this type of reaction leads to the depolymerization of lignin chain structure. Only transformation of the side chain such as C_γ-elimination is not included. Guaiacol (**9**) (for model dimers **1**–**4**) and veratraldehyde (**17**) (for model dimer **6**) were used as depolymerization products. Condensation/carbonization reactivity is shown as the yield of the THF-insoluble fraction.

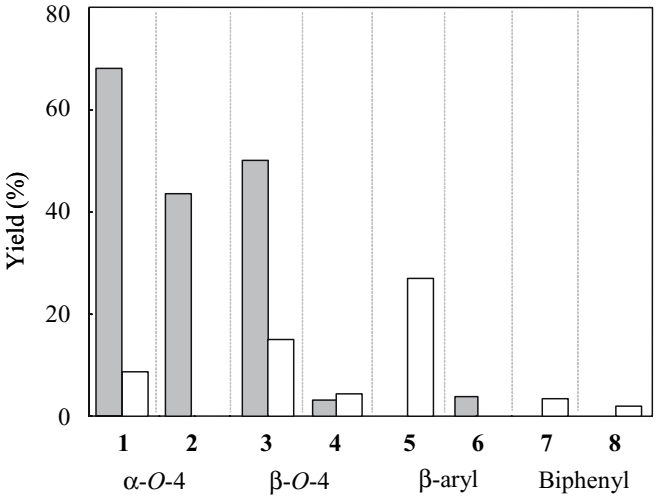

Fig. 9. Relative reactivity of substructure in lignin indicated by the model dimer study for depolymerization and condensation/carbonization at 400°C. *Shaded bars*, depolymerization (guaiacol yield for dimers **1**–**4**, veratraldehyde yield for dimer **6**), *open bars*, condensation/carbonization (yield of the THF-insoluble fraction)

These reactivities are quite different for model dimers. The *α-O*-4 type (**1** and **2**) and phenolic *β-O*-4 type (**3**) are expected to be very important substructures for deployerization of lignin chain structure at 400°C. The nonphenolic C_β-C_{aryl} type (**6**) and nonphenolic *β-O*-4 type (**4**) are the next important structures for depolymerization. Contrary to this, phenolic C_β-C_{aryl} type (**5**) is an important structure in the condensation/carbonization of lignin. Comparatively high yields of the THF-insoluble fraction observed in phenolic *β*-1 (**3**) and phenolic *β-O*-4 (**5**) types are considered to be related to the formation of the conjugated aromatic structures. Conjugated aromatic structure may enhance the condensation/carbonization reaction, although further study is necessary to understand the detail of the mechanism.

Conclusions

Primary pyrolysis reactions and relative reactivities for depolymerization and condensation/carbonization at 400°C were clarified for *α*-ether, *β*-ether, C_β-C_{aryl}, and biphenyl substructures by using a series of dimeric lignin model dimers. These results will be useful in understanding the whole lignin pyrolysis behavior in wood.

Acknowledgments This research was supported by a Grant-in-Aid for Scientific Research (C)(2)(No. 11660164, 1999.4–2000.3) and 21st COE program "Establishment of Sustainable Energy System" from the Ministry of Education, Culture, Sports, Science, and Technology, Japan.

References

1. Kawamoto H, Murayama M, Saka S (2003) Pyrolysis behavior of levoglucosan as an intermediate in cellulose pyrolysis: polymeriza-

tion into polysaccharide as a key reaction to carbonized product formation. J Wood Sci 49:469–473
2. Kawamoto H, Hatanaka W, Saka S (2003) Thermochemical conversion of cellulose in polar solvent (sulfolane) into levoglucosan and other low molecular-weight substances. J Anal Appl Pyrolysis 70:303–313
3. Kawamoto H, Saka S (2006) Heterogeneity in cellulose pyrolysis indicated from the pyrolysis in sulfolane. J Anal Appl Pyrolysis 76:280–284
4. Kawamoto H, Saito S, Hatanaka W, Saka S (2006) Catalytic pyrolysis of cellulose in sulfolane with some acidic catalysts. J Wood Sci DOI: 10.1007/s10086-006-0835-y
5. Ramiah MV (1970) Thermogravimetric and differential thermal analysis of cellulose, hemicellulose, and lignin. J Appl Polym Sci 14:1323–1337
6. Stahl E, Karig F, Brögmann U, Nimz H, Becker H (1973) Thermofractography of lignin and its use for rapid analysis on the ultra-micro-scale. Holzforschung 27:89–92
7. Karig VF, Stahl E (1974) Über den Einfluß der Thermolysebedingungen auf funktionelle Gruppen bei der Thermofraktographie von Ligninen. Holzforschung 28:201–203
8. Fenner RA, Lephardt JO (1981) Examination of the thermal decomposition of Kraft lignin by Fourier transform infrared evolved gas analysis. J Agric Food Chem 29:846–849
9. Jakab E, Faix O, Till F, Székely T (1995) Thermogravimetry/mass spectrometry study of six lignins within the scope of an international round robin test. J Anal Appl Pyrolysis 35:167–179
10. Jakab E, Faix O, Till F (1997) Thermal decomposition of milled wood lignins studied by thermogravimetry/mass spectrometry. J Anal Appl Pyrolysis 40–41:171–186
11. Haw JF, Schultz TP (1985) Carbon-13 CP/MAS NMR and FT-IR study of low-temperature lignin pyrolysis. Holzforschung 39:289–296
12. Domburg GE, Sergeeva VN, Zheibe GA (1970) Thermal analysis of some lignin model compounds. J Therm Anal 2:419–428
13. Domburg GE, Rossinskaya G, Sergeeva V (1974) Study of thermal stability of β-ether bonds in lignin and its models. Proceedings of the 4th International Conference on Thermogravimetric Analysis, 2:211–220
14. Domburg GE, Rossinskaya G, Dobele G (1975) Thermoanalytical study of model lignin compounds. V. Thermal decomposition of acetovanillone benzyl ether and pinoresinol. Koksnes Kimija 87–94
15. Klein MT, Virk PS (1981) Model pathways of lignin thermolysis. Report MIT-EL81-005
16. Brežný R, Mihálov V, Kváčik V (1983) Low temperature thermolysis of lignins. I. Reactions of β-*O*-4 model compounds. Holzforschung 37:199–204
17. Adler E (1977) Lignin chemistry – past, present and future. Wood Sci Technol 11:169–218
18. Nakatsubo F, Sato K, Higuchi T (1975) Synthesis of guaiacylglycerol-β-guaiacyl ether. Holzforschung 29:165–168
19. Kristersson P, Lundquist K (1980) A new synthetic route to lignin model compounds of the 1,2-diaryl-1,3-propanediol type. Acta Chem Scand B34:213–234
20. Li S, Lundquist K, Stomberg R (1993) Synthesis of 1,2-bis(3,4-dimethoxyphenyl)-1,3-propanediol starting from *trans*-1,3-bis(3,4-dimethoxyphenyl)-2,3-epoxy-1-propanone. Acta Chem Scand 47:867–871
21. Kratzl K, Vierhapper FW (1971) Synthese von ^{14}C-kernmarkierten Vanillinen und Bikreosolen. Monatsh Chem 102:425–430
22. Yaguchi T, Hosoya S, Nakano J, Satoh A, Nomura Y, Nakamura M (1979) Mechanism of rapid delignification during alkaline cooking with addition of tetrahydroanthraquinone. Mokuzai Gakkaishi 25:239–240
23. Gierer J, Lenic J, Norén I, Szabo-Lin I (1974) Lignin chromophores. Part I. Synthesis of chromophores of the 2,4′- and 4,4′-dihydroxystilbene types. Acta Chem Scand B28:717–729
24. Szabo-Lin I, Teder A (1976) Absorption bands in the electronic spectra of lignin model compounds. Part 2. Stilbenes. Sven Papperstidn 5:153–156